Topography of Diphtheria Toxin A Chain Inserted into Lipid Vesicles†

Masatoshi Hayashibara and Erwin London*

Department of Biochemistry and Cell Biology and Department of Chemistry, Stony Brook University, S.U.N.Y., Stony Brook, New York 11794-5215

Received August 18, 2004; Revised Manuscript Received November 23, 2004

ABSTRACT: The membrane-inserting T domain of diphtheria toxin aids the low-pH-triggered translocation of the catalytic A chain of the toxin across endosomal membranes. To evaluate the role of the isolated A chain in translocation, the topography of isolated A chain inserted into model membrane vesicles was investigated using a mixture either of dioleoylphosphatidylcholine (DOPC) and dioleoylphosphatidylglycerol (DOPG) or of dimyristoleoylphosphatidylcholine (DMoPC) and DOPG. The latter mixture was previously found to promote deep insertion of the T domain. A series of single Cys mutants along the A chain sequence were labeled with bimane or BODIPY groups. After A chain insertion into model membranes, the location of these groups within the lipid bilayer was determined via bimane fluorescence emission λ_{max}, binding of externally added anti-BODIPY antibodies, and a novel technique involving the comparison of the quenching of bimane fluorescence by aqueous iodide and membrane-associated 10-doxylnonadecane. The results show that in both DOPC- and DMoPC-containing bilayers, membrane-inserted residues all along the A chain sequence occupy shallow locations that are relatively exposed to the external solution. There were only small differences between A chain topography in the two different types of lipid mixtures. However, the behavior of the A chain in the two different lipid mixtures was distinct in that it strongly oligomerized in DMoPC-containing vesicles as judged by Trp fluorescence. In addition, A chain selectively induced fusion of the DMoPC-containing vesicles, and this may aid oligomerization by increasing the A chain/vesicle ratio. Fusion may also explain why A chain also selectively induced leakage of the contents of DMoPC-containing vesicles. We propose that isolated A chain is unlikely to be inserted in a transmembrane orientation, and thus its interaction with the T domain is likely to be critical for properly orienting the A chain within the bilayer in a fashion that allows translocation.

Diphtheria toxin (DT)[1] is a protein toxin secreted by *Corynebacterium diphtheriae*. After proteolytic processing, the toxin consists of two polypeptide chains, A (21 kDa) and B (37 kDa), that are joined by a disulfide bond. The A chain is identical to the catalytic (C) domain of the protein, while the B chain consists of two domains, the receptor binding domain (R) and the transmembrane (T) domain (*1*, *2*). After entry into endosomes via receptor-mediated endocytosis, a conformational change triggered by the low pH of the endosomal lumen renders the toxin hydrophobic. This allows the toxin to penetrate the endosomal membrane and translocate its A chain into the cytosol. The final release of the A chain may follow reduction of the disulfide linking it to the T domain, perhaps with the aid of cytosolic proteins (*3*). Once in the cytosol, the A chain catalyzes the ADP-ribosylation of the diphthamide residue of elongation factor 2, which inhibits protein synthesis and leads to cell death (*4*). Study of this system may allow us to better elucidate the poorly understood process of protein translocation across biological membranes.

Although it may be aided by cytosolic proteins, A chain translocation can also be observed in a cell-free system, suggesting that the toxin alone possesses the ability to penetrate and cross lipid bilayers (*5*−*8*). Nevertheless, the exact mechanism of translocation remains unclear (*6*). The T domain clearly has a key role in promoting the translocation of the A chain. It forms a pore through which the A chain may pass, may interact with the A chain so as to shield hydrophilic sites on the A chain from contact with lipid, and/or may act as a chaperone that interacts with hydrophobic sites on the partly unfolded A chain and prevents its folding during translocation (*9*−*13*). The role of the A chain itself in the translocation process is also unclear. Early studies showed that the A chain is able to tolerate denaturing conditions, suggesting the possibility that it might be able to unfold during translocation and then refold (*14*, *15*). Cross-

* To whom correspondence should be addressed. Phone: 631-632-8564. Fax: 631-632-8575. E-mail: erwin.london@stonybrook.edu.

† This work was supported by NIH Grant GM 31986.

[1] Abbreviations: ABD-PE, *N*-(7-aminobenz-2-oxa-1,3-diazol-4-yl)-1,2-dihexadecanoyl-*sn*-glycero-3-phosphoethanolamine; biocytin, ϵ-*N*-biotinyl-L-lysine; BODIPY, 4,4-difluoro-4-bora-3a,4a-diaza-*s*-indecene; BODIPY-IA, BODIPY-FL C1-IA, *N*-[(4,4-difluoro-5,7-dimethyl-4-bora-3a,4a-diaza-*sn*-indecene-3-yl)methyl]iodoacetamide; CD, circular dichroism; DMoPC, 1,2-dimyristoleoyl-*sn*-glycero-3-phosphocholine; 10-DN, 10-doxylnonadecane, 4,4-dimethyl-2,2-dinonyl-3-oxazolidinyloxy, free radical; DOPC, 1,2-dioleoyl-*sn*-glycero-3-phosphocholine; DOPG, 1,2-dioleoyl-*sn*-glycero-3-phosphoglycerol; DT, diphtheria toxin; DTT, dithiothreitol; FPLC, fast protein liquid chromatography; FRET, fluorescence resonance energy transfer; FTIR, Fourier transform infrared spectroscopy; IPTG, isopropyl-β-D-thiogalactopyranoside; LUVs, large unilamellar vesicles; LB, Luria−Bertani; NBD-PE, *N*-(7-nitrobenz-2-oxa-1,3-diazol-4-yl)-1,2-dihexadecanoyl-*sn*-glycero-3-phosphoethanolamine; PMSF, phenylmethylsulfonyl fluoride; OD, optical density; rhodamine-PE, *N*-(lissamine rhodamine B sulfonyl)-1,2-dioleoyl-*sn*-glycero-3-phosphoethanolamine; SUVs, small unilamellar vesicles; TM, transmembrane; WT, wild type.

10.1021/bi0482093 CCC: $30.25
Published on Web 01/20/2005

linking studies indicated that in membrane-inserted whole DT, the A chain was accessible to the hydrophobic part of the bilayer (*16*−*18*). Later studies showed that at low pH the isolated A chain undergoes partial unfolding (*11*), perhaps forming a molten globulelike conformation, and that in the low-pH conformation it has the ability to bind to (and to some degree insert into) lipid bilayers (*11*, *17*). Exposure to neutral pH resulted in the release of the isolated A chain from the bilayer and its refolding into the native conformation (*11*, *19*). A similar refolding and release of A chain from model membranes could be observed, using whole toxin inserted at low pH into bilayers, upon pH neutralization and cleavage of the disulfide attaching A chain to the rest of the toxin by DTT (*20*). Additional studies both in cells (*21*, *22*) and in model membranes (*7*, *23*) indicated that the A chain must be unfolded in order to undergo efficient translocation.

Although these studies suggested that the A chain could interact with the lipid bilayer during at least some stages of translocation, they did not clarify the degree to which the A chain participates in the translocation process or the precise nature of A chain interaction with lipid. To clarify the capacity of the isolated A chain to interact with lipid and contribute to its own translocation, we undertook a detailed analysis of the topography of model membrane-bound A chain in this study. The results indicate that at least most of the isolated A chain does not penetrate deeply into the bilayer. This is true even under conditions previously shown to promote deep insertion of the T domain. As a consequence, it is likely that part of the role of the T domain is to help orient membrane-inserted A chain for translocation.

EXPERIMENTAL PROCEDURES

Materials. Dimyristoleoylphosphatidylcholine (DMoPC), dioleoylphosphatidylcholine (DOPC), dioleoylphosphatidylglycerol (DOPG), NBD-PE, and rhodamine-PE were purchased from Avanti Polar Lipids (Alabaster, AL). Lipid concentrations were determined as described previously (*24*) or, for labeled lipids, on the basis of their extinction coefficients (*25*). 10-Doxylnonadecane (10-DN) was purchased from Aldrich (Milwaukee, WI) (discontinued, contact authors for availability). Its concentration was determined by absorbance at 231 nm (*26*). (However, recent studies suggest 10-DN absorbance at visible wavelengths gives a more accurate measure of concentration (*27*).) Biocytin hydrochloride and bovine serum albumin were purchased from Sigma (St. Louis, MO). Monochlorobimane, BODIPY-FL C1-IA (BODIPY-IA), rabbit anti-BODIPY-FL IgG, and streptavidin-BODIPY-FL conjugate (BODIPY-streptavidin, custom order) were purchased from Molecular Probes (Eugene, OR). *Eco*RI, *Nde*I, *Pfx* DNA polymerase, and synthetic oligonucleotides were purchased from Invitrogen (Carlsbad, CA). Shrimp alkaline phosphatase was purchased from Roche Applied Science (Indianapolis, IN). Source 15Q and Sepharose CL-4B resins were purchased from Amersham Pharmacia Biotech (Piscataway, NJ). All other chemicals were reagent grade.

Site-Directed Mutagenesis. DT A chain DNA cloned into the pET-28a plasmid was used as a template for mutagenesis. The original template consisted of A chain residues 1−189 with the E148S substitution, which abolishes toxicity (*28*). A chain numbering followed that of native DT (*29*). The native Cys at residue 186 was replaced with Ala by mutagenesis to prepare a Cys-less template for the introduction of single Cys mutations at various positions. To replace Cys 186 with Ala and to introduce Cys residues, two-step PCR (overlap extension) was carried out on an Eppendorf Mastercycler Personal PCR system using *Pfx* DNA polymerase as described previously (*30*, *31*). The final PCR product and the pET-28a vector were cleaved by the *Eco*RI and *Nde*I restriction enzymes, and the digested vector was dephosphorylated with alkaline phosphatase. The polynucleotides were purified by agarose-gel electrophoresis and then the digested PCR product and the linear vector were ligated by T4 DNA ligase (as described by the manufacturer for the pET system (Novagen, Madison, WI)). Finally, *E. coli* XL-1 Blue cells were transformed by electroporation with the resulting plasmid (*32*). The A chain inserts were sequenced to verify that only the desired mutation was introduced (Proteomics Center, Stony Brook, NY). Plasmids with the confirmed mutations were transformed into an *E. coli* BL 21 cell strain (used for A chain expression) by heat shock (*32*).

Protein Expression and Purification. A chain proteins were expressed and isolated from *E. coli* strains similarly to previous procedures used for the T domain (*33*). A 21 residue sequence with six His residues ("His_6 tag") was attached to the N-terminus of the A chain (*34*). LB media with 50 μg/mL kanamycin was used to select plasmid-containing bacteria. Overnight starter cultures were prepared and diluted 50-fold with 1−2 L of media to prepare large-scale cultures. After 2 h, expression was induced with IPTG (500 mg/l), and after 3 h, further incubation cells were collected by centrifugation. A cell extract was prepared by sonication and then adsorbed for 40 min onto 0.5 mL of Talon metal affinity resin (CLONTECH, Palo Alto, CA) to bind the His_6-tagged A chain. After transfer of the resin to a column, the resin was washed with 15 mL of sonication buffer (100 mM NaCl, 20 mM Tris-Cl, pH 8), followed by three individual 1 mL aliquots of elution buffer (100 μM PMSF, 100 mM imidazole, 100 mM NaCl, 20 mM Tris-Cl, pH 8). Most of the A chain eluted in the last two aliquots of elution buffer. The A chain-containing fractions were pooled, diluted to 10 mL with 20 mM Tris-Cl, pH 8, and then subjected to FPLC on a 3 mL Source-Q anion-exchange column (Amersham Pharmacia Biotech, Piscataway, NJ), eluting at a rate of 0.5 mL/min with a gradient containing 20mM Tris-Cl pH 8 and an increasing concentration of NaCl (0−500 mM). A chain eluted between 350 and 500 mM NaCl. Purity was checked by SDS-polyacrylamide gel electrophoresis using a Phast-system electrophoresis system (Amersham Pharmacia Biotech, Piscataway, NJ) and visualized by Coomassie Brilliant Blue staining. Final purity appeared to be >95%. Purified fractions were stored at 4 °C. Concentrations of A chain were determined by the Bradford method (*35*) using the Coomassie Brilliant Blue G-250 dye (Bio-Rad, Hercules, CA) and bovine serum albumin as a standard. (Concentrations determined by absorbance at 280 nm, assuming an extinction coefficient of 25 900 cm^{-1} M^{-1} calculated from the published extinction coefficients of Trp and Tyr residues (*36*) and an A chain formula weight of 22 891 Da, were 10% higher than those derived from the Bradford assay.) The purified A chain was typically stored at a concentration of 2−17 mg/mL (by Bradford assay). As judged by gel electrophoresis, some

single Cys mutants formed a significant amount (but <50%) of apparently disulfide-linked dimers. Proteins were all treated with dithiothreitol (DTT) prior to labeling to reduce any disulfides (see below).

Fluorescence Labeling of A Chain Mutants. A chain was labeled with BODIPY-IA and monochlorobimane similarly to the procedure described previously (*37*). To label, 1 μL of 25 μM BODIPY-IA dissolved in dimethyl sulfoxide (6:1 mol ratio of probe:protein) or 1 μL of 57 mM monochlorobimane dissolved in ethanol (13:1 mol ratio of probe: protein) was added to 100 μg of A chain and diluted to 1 mL with 150 mM NaCl, 10 mM Tris-Cl, pH 8 (Tris buffer pH 8). Samples were then incubated at room temperature for 1 h. Free labeling reagent was removed by overnight dialysis (using 8000-MW-cutoff tubing) against 4 L of 140 mM NaCl, 10 mM Tris-Cl, pH 8, at 4 °C with one change of dialysis buffer. In all cases, specific labeling of Cys residues was confirmed by comparing the labeling to that of a Cys-less A chain mutant. Labeling of Cys was at least 15-fold greater than the labeling of the Cys-less protein for bimane and at least 22-fold greater than Cys-less protein for BODIPY. It was assumed that the concentration of labeled A chain was not affected by dialysis. This assumption was confirmed by a control dialysis (less than 8% decrease of protein concentration as judged by absorbance at 280 nm).

Fluorescence Measurements. Fluorescence was measured with a Spex 212 Fluorolog spectrophotometer operating in ratio mode (*31*). Unless otherwise noted, measurements were made in semimicro quartz cuvettes with an excitation path length of 10 mm and an emission path length of 4 mm. The excitation and emission slit widths used were 2.5 and 5 mm, respectively. Trp fluorescence was measured with an excitation wavelength of 280 nm. Emission spectra of Trp were measured from 300 to 400 nm at a rate of 1 nm/s. Bimane fluorescence was measured with an excitation wavelength of 375 nm. Bimane emission spectra were measured from 420 to 520 nm at a rate of 1 nm/s. BODIPY fluorescence was measured with an excitation wavelength of 485 nm and an emission wavelength of 515 nm. In all cases, background intensities from samples lacking protein were subtracted from the intensities measured in the A chain-containing samples. Fluorescence resonance energy transfer (FRET) was evaluated as described previously. The enhancement of rhodamine fluorescence relative to NBD fluorescence was evaluated by the ratio of the emission intensity at 590 relative to 535 nm, with excitation at 460 nm (*38*). All experiments were carried out at room temperature unless otherwise noted.

Preparation of Model Membrane-Incorporated A Chain. Samples containing A chain were incorporated into small unilamellar vesicles (SUVs). Stock solutions of 70% DMoPC/30% DOPG or 70% DOPC/30% DOPG (mol/mol) SUVs with a final concentration of 10 mM lipid were prepared using a bath sonicator (Laboratories Supply Co., Hicksville, NY) as previously described (*34*). SUVs were prepared in 150 mM NaCl, 6.7 mM Tris-Cl, 167 mM sodium acetate, pH 4.5 (acetate buffer pH 4.5). In general, lipid vesicles were made within 1 day of use and stored at 4 °C. Typically, a 32 μL aliquot of SUVs was added to a cuvette containing 736 μL of acetate buffer pH 4.5. To this, 32 μL of 100 μg/mL fluorescently labeled A chain was added while vortexing and then the sample was incubated for 30 min before measuring fluorescence. The final volume of each sample was 800 μL. For bimane-labeled samples, fluorescence emission spectra were then measured as described above. For the BODIPY-labeled samples, anti-BODIPY quenching was performed as described previously (*33*), except that for all samples, A chain, lipid, and antibody concentrations were decreased 2-fold to eliminate the turbidity observed after antibody addition.

Effect of Removal of His_6 Tag. In some control experiments, N-terminal His_6 tag was removed from A chain mutants using thrombin as described previously (*33*). After the removal of the His_6 tag, four vector-encoded residues were left at the N-terminus (*34*). Digested proteins were subsequently separated from any residual protein with undigested His_6 tag using a TALON affinity column. Removal of the tag was confirmed by SDS-polyacrylamide gel electrophoresis. After bimane labeling, we found that labeled G1C and T111C had similar bimane emission maxima with and without the His_6 tag in both acetate buffer pH 4.5 and Tris buffer pH 8. In a more detailed experiment, a labeled S30C mutant showed the same pH dependence of bimane fluorescence in solution with and without the His_6 tag. In additional controls, we found that the pH dependence of fluorescence in the presence of DOPG/DOPC SUVs (see below) was similar with and without the His_6 tag for A chain with a bimane-labeled L136C residue and for wild-type A chain labeled on Cys 186. Since the His_6 tag had no effect on A chain behavior under our experimental conditions, it was not removed in subsequent experiments.

pH Titration of the Fluorescence of A Chain. The fluorescence of bimane-labeled residues or of the native Trp of the A chain was monitored during acidification of the samples from pH 8 to pH 3 (*11*). Quartz cuvettes with excitation and emission path lengths of 10 mm were used to allow monitoring of pH with a normal size glass electrode. A 1.75 mL solution containing A chain diluted to 4 μg/mL with either Tris buffer pH 8 or the desired concentration of lipid dispersed in Tris buffer pH 8 was used as the starting solution. (For these experiments, stock solutions of 10 mM 7:3 DMoPC/DOPG or 7:3 DOPC/DOPG (mol/mol) SUVs were prepared by sonication as described above except that Tris buffer pH 8 was used instead of acetate buffer pH 4.5.) Background samples were prepared similarly, except that the A chain was not added. Aliquots (1−8 μL) of 1 M acetic acid or 1 M HCl (below pH 4.2) were added stepwise. Each sample was vortexed briefly after adding an aliquot of acid and incubated for 5 min before measuring pH and fluorescence. It should be noted that these results were not affected by dimerization of the A chain via disulfide formation. Single Cys mutants remained relatively monomeric (<10% dimers)-during the maximum of 1 day of storage at 4 °C after DTT treatment and FPLC purification but prior to the experiments, as confirmed by SDS-polyacrylamide gel electrophoresis.

Relative Depth of Bimane-Labeled Residues. Iodide quenching of bimane-labeled residues was evaluated by comparing the fluorescence intensity of samples in the absence of iodide to that in its presence. To do this, the fluorescence of samples containing SUV-inserted A chain dispersed in 800 μL of acetate buffer pH 4.5, or background samples without protein, prepared as described above, was measured. At this step, samples contained 400 μM 7:3 DMoPC/DOPG or 7:3 DOPC/DOPG (mol/mol) plus 4 μg/mL A chain. Fluorescence was remeasured 30 min after the addition of 50 μL of an aqueous

solution containing 1.7 M KI and 0.85 mM $Na_2S_2O_3$ (*39*). This gave a final KI concentration of 100 mM. (A 2 M stock solution of KI containing 1 mM $Na_2S_2O_3$ showed no significant absorption between 280 and 550 nm over two months, indicating no formation of I_2 or I_3^-.) 10-DN quenching of bimane-labeled residues was evaluated by comparing the fluorescence intensity of samples in the absence of 10-DN to that in its presence. Stock solutions of 7:3 DMoPC/DOPG or 7:3 DOPC/DOPG (mol/mol) SUVs with a lipid concentration of 10 mM were prepared by sonication as described above. Stock solutions of SUVs containing 10-DN were prepared similarly, except that the desired amount of 10-DN dissolved in ethanol was added to the lipids in chloroform; after drying in an N_2 stream, the lipid was suspended in Tris buffer pH 8 and sonicated as briefly as possible to allow the formation of SUVs (less than 15 min) while avoiding damaging the 10-DN nitroxide group. The final concentration of 10-DN in the lipid bilayers was 7.2 mol % for DMoPC/DOPG vesicles and 9.1 mol % for DOPC/DOPG vesicles. These values kept the ratio of 10-DN to hydrophobic volume similar in the two different lipid compositions (*26*). For the 10-DN quenching experiments, 32 μL of 100 μg/mL bimane-labeled protein (or buffer alone in background samples) were diluted to 768 μL with acetate buffer pH 4.5, and to adjust for any differences in protein concentrations due to pipetting error bimane fluorescence was measured prior to the addition of the aliquot of SUVs. Then, 32 μL of SUV stock solutions with or without 10-DN were added to the samples, while vortexing, and fluorescence was remeasured after a further 30 min of incubation. Final concentrations were 4 μg/mL A chain plus 400 μM phospholipid and the desired amount of 10-DN. The final pH in these mixtures was pH 4.5. In these experiments, bimane fluorescence was measured at an excitation wavelength of 375 nm and an emission wavelength of 467 nm.

Size Exclusion Chromatography. SUVs containing 9 mM lipid composed of 7:3 (mol/mol) DMoPC/DOPG or 7:3 DOPC/DOPG (both lipid mixtures being labeled with 0.14 μM rhodamine-PE) with (or when desired without) 450 μg/mL of A chain were prepared in pH 4 buffer (1 volume of Tris buffer pH 8 plus 0.017 volume of 1 M acetic acid and 0.0022 volume of 1 M HCl) as in previous sections, except that protein and lipid were coincubated for 1 h. [In one experiment to examine the effect of pH neutralization, after incubation at low pH, an aliquot of 1 M NaOH (about 7 μL) was added in order to adjust the pH to 8 and the sample was incubated for 1 h further.] Next, 500 μL aliquots of each sample were chromatographed on a Sepharose CL-4B column (41 cm length $\times$ 0.75 cm diameter). The column was preequilibrated and eluted with the appropriate buffer for each sample. Fractions of approximately 900 μL were collected and rhodamine fluorescence in each was measured at an excitation wavelength of 565 nm and an emission wavelength of 585 nm to detect SUV elution. The concentration of A chain in each fraction was monitored by measuring the native Trp fluorescence at an excitation wavelength of 280 nm and an emission wavelength of 335 nm.

"Pore" Formation Estimated from Biocytin Leakage. To estimate the pore formation/leakiness-inducing activity of A chain or T domain, biocytin was entrapped into SUVs. SUVs containing 10 mM lipid composed of 70% DMoPC/30% DOPG (mol/mol) or 70% DOPC/30% DOPG (mol/mol) were prepared using a bath sonicator as described above, except that lipids were dispersed in the presence of 180 μM biocytin. Biocytin outside the SUVs was then removed by overnight dialysis (using 8000-MW-cutoff dialysis tubing) at 4 °C against 4 L of Tris buffer pH 8 with one change of dialysis buffer. A 16 μL aliquot of dialyzed SUVs with entrapped biocytin and 2 μL from a 20 μg/mL solution of BODIPY-streptavidin dissolved in water were added into 778 μL of acetate buffer pH 4.5, and BODIPY fluorescence was measured as described above. After 10 min, 4 μL of 400 μg/mL protein (diluted from the stock solution with Tris buffer pH 8), or in mock experiments Tris buffer pH 8, was added to the samples and BODIPY fluorescence was measured after 30 min. The mock sample showed less than a 5% increase in BODIPY fluorescence. After 90 min, to see if release of biocytin was complete and/or if additional protein could induce further release, a second addition of protein at twice the concentration as in the first addition was added for both A chain and T domain samples, and the fluorescence enhancement was measured after an additional 30 min of incubation.

Permeability of Iodide Ion through Lipid Bilayers Tested by NBD Fluorescence Quenching of Internally Labeled SUVs. To determine the conditions in which iodide would pass through a lipid bilayer, it was necessary to prepare vesicles in which iodide-sensitive NBD groups were restricted to the interior of the bilayer. To do this, the destruction of NBD fluorescence from the external leaflet of labeled SUVs was performed by the method of McIntyre and Sleight (*40*). SUVs composed of 7:3 DOPC/DOPG (mol/mol) with 0.1 mol % NBD-PE were prepared in Tris buffer pH 8 by sonication at a 10 mM lipid concentration as described above. A solution of 1 M sodium dithionite ($Na_2S_2O_4$) was freshly prepared in Tris buffer pH 8, and a 5.6 μL aliquot was immediately added to 394.4 μL of the SUVs diluted in Tris buffer pH 8 (pH 8 being used to minimize self-decomposition of dithionite) to give a lipid concentration of 200 μM. After a 30 min incubation, the sample was placed in 8000-MW-cutoff dialysis tubing and dialyzed for 4 h at 4 °C against 4 L of Tris buffer pH 8. NBD fluorescence of both dithionite-treated and untreated samples was measured with an excitation wavelength of 460 nm and an emission wavelength of 534 nm both before and after the dialysis step. This showed that no significant change in fluorescence occurred during dialysis. A 400 μL aliquot of the SUV-containing sample (or a 400 μL aliquot of a sample untreated with dithionite and not dialyzed) was then diluted with 400 μL of Tris buffer pH 8 or acetate buffer pH 4.5. (Tris buffer in the 400 μL aliquot of the SUV-containing sample increased the pH of the acetate buffer (pH 4.5) by less than 0.1 unit due to the high acetate concentration in the latter buffer.) NBD fluorescence was measured; then, 141 μL of a solution containing 2 M KI and 1 mM sodium thiosulfate ($Na_2S_2O_3$) was added, and fluorescence was monitored for 45 min. The value of fluorescence after 30 min, by which time it had nearly stabilized, was used to estimate iodide permeability. Control experiments with KCl demonstrated that the changes in fluorescence were due to iodide quenching and not a change in salt concentration (data not shown).

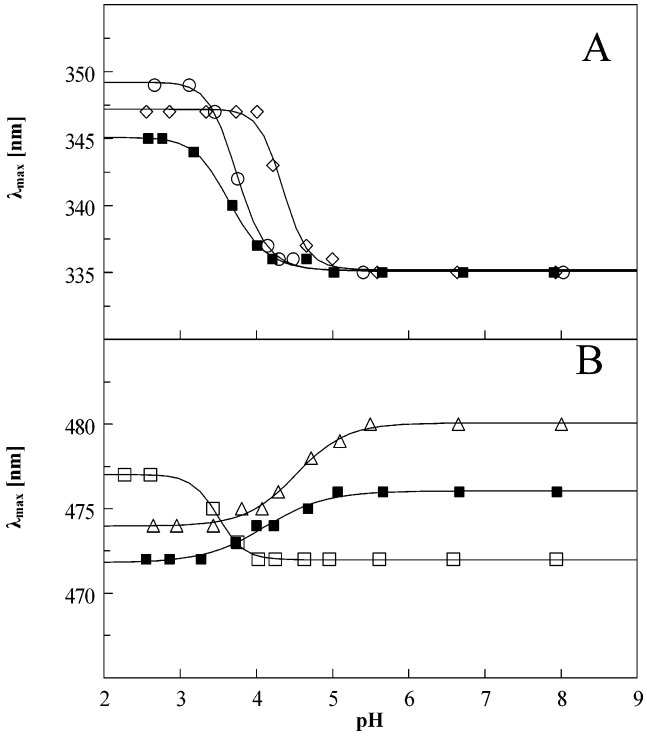

FIGURE 1: pH titration of native Trp fluorescence of unlabeled A chain and bimane fluorescence of labeled A chain in solution. (A) pH dependence of native Trp fluorescence of Cys-less (*open circles*), L136C (*open diamonds*) mutants, and wild-type (*filled squares*) A chain in solution. (B) pH dependence of bimane fluorescence of labeled G1C (*open squares*) and E162C (*open triangles*) mutants and wild-type [labeled on C186] (*filled squares*) A chain in solution. Initial samples contained 0.18 μM A chain in 10 mM Tris-Cl, 150 mM NaCl, pH 8.

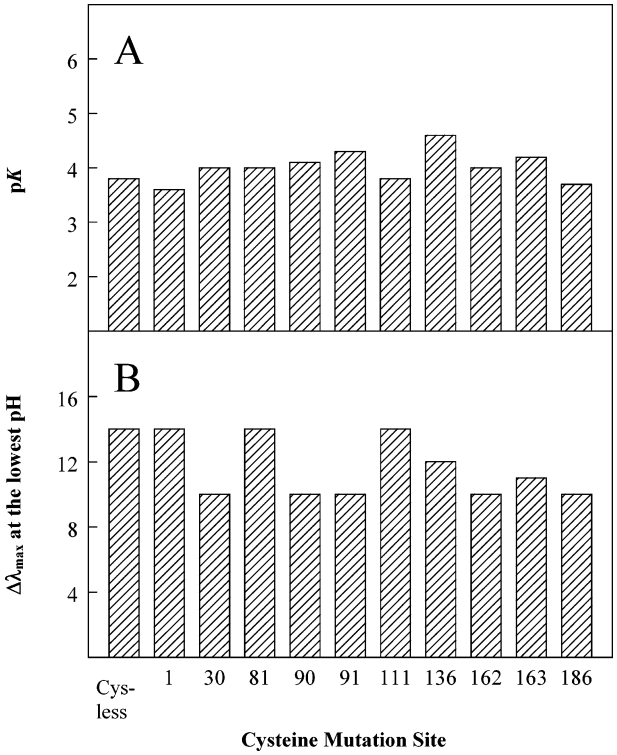

FIGURE 2: Apparent p*K* for low-pH-induced conformational transition and pH-induced shift in Trp emission λ_{max} in solution determined from titration experiments. Titration experiments carried out as in Figure 1. (A) apparent conformational p*K* detected by measurement of native Trp fluorescence of unlabeled A chain during pH titration. p*K* was defined as the estimated midpoint of pH-induced λ_{max} shift. (This value may be slightly shifted from the true midpoint, as average λ_{max} is weighted by the quantum yield of the native and low-pH conformations.) (B) $\Delta\lambda_{max}$ of native Trp fluorescence. $\Delta\lambda_{max}$ was defined as the difference between λ_{max} at the lowest and highest pH. In solution, the Trp emission maximum of WT A chain at neutral pH was 335 nm, while the averaged value for Cys-less and single-Cys mutants was 336 $\pm$ 1 nm (data not shown). Number on *x*-axis indicates position of Cys residue in A chain; 186 indicates wild-type A chain.

RESULTS

Effect of Mutagenesis on Neutral- and Low-pH Conformation of A Chain in Solution. To study the topography of membrane-inserted A chain, a Cys-less A chain (C186A) was constructed from wild-type (WT) A chain. Then, in different mutants, G1, S30, V81, K90, V91, T111, L136, E162, or L163 was replaced by a single Cys residue. One reason that these residues were chosen is that as visualized by the Rasmol program, they appear to be exposed to solution as judged from the crystal structure of the native A chain (within whole toxin) (*2*) and thus should be accessible to labeling. A second reason that they were chosen was to allow for the scanning of conformational changes and lipid interaction at residues throughout the A chain sequence, including hydrophilic α-helices (CH2 and CH7 (residues 30 and 186, respectively)), hydrophilic segments (at the N-terminus of A chain (residue 1) and the loop between CH4 and CH5 (residue 111)), and most importantly within the β-sheets that have the potential to form transmembrane structures (CB4, CB5, CB6, and CB8 (residues 81, 90−91, 136, and 162−163, respectively)) (*23*).

Control experiments were first performed to examine A chain behavior as a function of pH and test whether A chain behavior was altered by introduction of single Cys and/or labeling of Cys residues. First, the pH dependence of the fluorescence of native A chain Trp (located in the loops between CH2 and CB3 (W50) and between CB7 and CB8 (W153)) was evaluated. Representative titrations are shown in Figure 1A. In agreement with previous studies, at low pH, there is strong red-shifting of Trp fluorescence (*11*). This reflects an increased exposure of Trp to solution due to partial unfolding of the native conformation (*11*). As summarized in Figure 2A, the midpoint pH (apparent "p*K*" values) of the conformational transition (i.e., the pH at which the change in Trp emission λ_{max} was midway between that at neutral and low pH values) and the change in Trp emission λ_{max} at low pH were very similar for wild-type and single Cys mutants (Figure 2B). The similarity of wild-type and mutant values shows that the stability of the native conformation was not severely disturbed by mutagenesis. Next, the pH dependence of bimane fluorescence of bimane-labeled proteins was evaluated. Representative titrations are shown in Figure 1B. As summarized in Figure 3A, the p*K* of the low-pH conformational transition in solution (striped bars) for bimane-labeled A chain was similar to that for unlabeled A chain. This suggests that, in general, bimane labeling did not markedly perturb the pH-induced conformational transition. However, the nature of the fluorescence change at low pH strongly depended upon bimane position, as illustrated in Figures 1B and 3B. As shown in Figure 3B (striped bars), residues nearer to the N-terminal tended to red-shift at low pH, whereas those closer to the C-terminal tended to blue-shift. These shifts presumably reflect the difference in

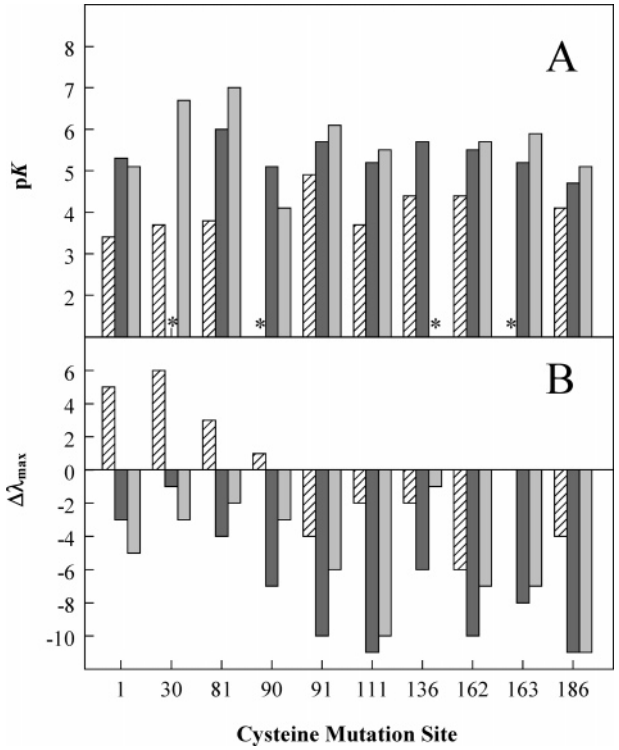

FIGURE 3: Apparent p*K* for low-pH-induced conformational transition and pH-induced shift in bimane emission λ_{max} determined from titration experiments. Titration experiments carried out as in Figure 1. (A) apparent p*K* of bimane fluorescence for labeled A chain. (B) $\Delta\lambda_{max}$ of bimane fluorescence, defined as in caption of Figure 2. Samples of A chain were prepared (*striped bars*) in solution as described above or as above but in the presence of SUVs composed of (*dark gray bars*) 7:3 DMoPC/DOPG (mol/mol) or (*light gray bars*) 7:3 DOPC/DOPG (mol/mol). Lipid concentration was 400 μM. Asterisks indicate cases in which p*K* could not be estimated due to the small degree or lack of shift in emission maxima at low pH. $\Delta\lambda_{max}$ for C136 in solution was 0. At pH 8 in the titration experiments, the bimane emission maxima values for different labeled Cys in the absence of lipid were as follows: C1, C30, C81, 472 nm; C90, 470 nm; C91, C111, 477 nm; C136, 474 nm; C162, 480 nm; C163, 473 nm; C186, 476 nm. Duplicate samples prepared at pH 8 in solution gave very similar emission maxima. In most cases, at pH 8, λ_{max} in the presence of lipid was similar to that in its absence, although some mutants showed slightly blue-shifted fluorescence in the presence of lipid (not shown).

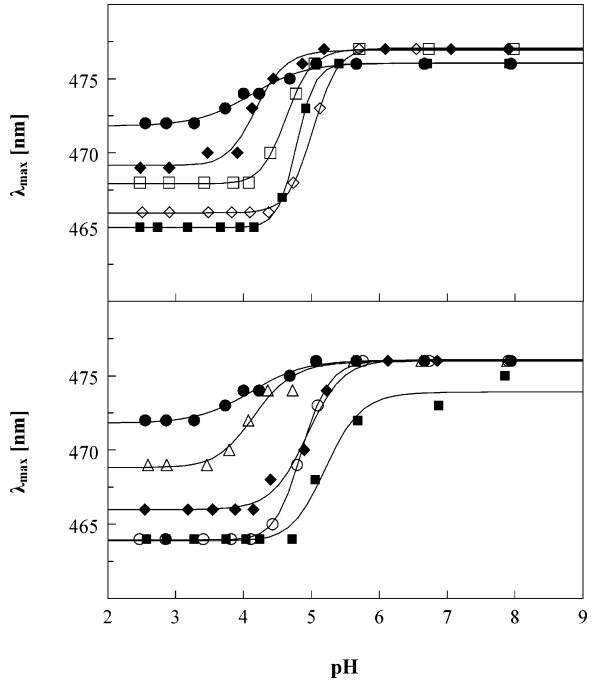

FIGURE 4: Effect of lipid concentration upon A chain binding to lipid evaluated from pH titration of bimane fluorescence with or without DMoPC/DOPG or DOPC/DOPG vesicles. Top: pH dependence of bimane fluorescence of labeled 0.18 μM wild-type A chain with various concentrations of 7:3 DMoPC/DOPG (mol/mol) SUVs. Filled circles: in solution. Filled diamonds, open squares, filled squares, open diamonds: with 40, 200, 400, and 600 μM lipid, respectively. Bottom: pH dependence of bimane fluorescence of 0.18 μM labeled wild-type A chain with various concentrations of 7:3 DOPC/DOPG (mol/mol) SUVs. Filled circles: in solution. Open triangles, filled diamonds, open circles, and filled squares: with 5, 40, 80, and 400 μM lipid, respectively. Titration experiments carried out as described in Figure 1.

polarity of the local environment around bimane in the folded state at neutral pH relative to the more unfolded state at low pH. Local environment can vary from residue to residue in a folded state. A position-dependent local environment is also likely to be present for A chain residues at low pH because previous studies have shown that the A chain forms a partially unfolded (i.e., molten-globule-like) conformation rather than a totally unfolded ("random coil") conformation at low pH (*11*). Molten-globule-state proteins retain a compact structure, albeit relatively disordered in terms of tertiary structure. Thus, from Figure 3B it appears that at low pH the residues in the N-terminal half of the protein tend to become more exposed to a polar environment (presumably the aqueous solution), while those at the C-terminal half become less exposed to a polar environment.

Topography of A Chain Inserted Into Model Membrane Vesicles. Previous studies have shown that the isolated A chain spontaneously inserts into lipid vesicles at low pH (*11*). We next investigated the conformation and topography of vesicle-inserted A chain. A chain was inserted into small unilamellar vesicles (SUVs) with two different lipid compositions: 70% DOPC/30% DOPG and 70% DMoPC/30% DOPG (mol:mol). These compositions were chosen because previous studies have shown that the T domain of diphtheria toxin inserts shallowly into DOPC/DOPG vesicles but deeply into DMoPC/DOPG vesicles (*24*, *33*).

Figure 4 shows the effect of lipid concentration upon the pH dependence of λ_{max} of bimane emission. As shown for labeled wild-type protein in Figure 4, addition of SUVs affects λ_{max} only at low pH, as expected from previous studies showing that the A chain only interacts with lipid vesicles at low pH (*11*). The effect of lipid at low pH was dependent on lipid concentration and was half-maximal at roughly 100 μM DMoPC/DOPG (Figure 4, top) or 50 μM DOPC/DOPG (Figure 4, bottom). To obtain relatively complete A chain binding, 400 μM lipid was used in most subsequent experiments.

Bimane fluorescence of labeled A chain single Cys mutants in the presence of lipid vesicles was then compared to that of labeled A chain in solution. As shown in Figure 3A (filled bars), the p*K* of the conformational transition increased by about 1−2 pH units relative to that in the absence of lipid in the presence of enough lipid to fully bind to the A chain. The effect of lipid is in agreement with previous studies (*11*) and reflects the fact that since only the unfolded conformation binds lipid, addition of lipid shifts the conformational equilibrium to favor unfolding. The larger increases in p*K* values for a couple of labeled mutants may

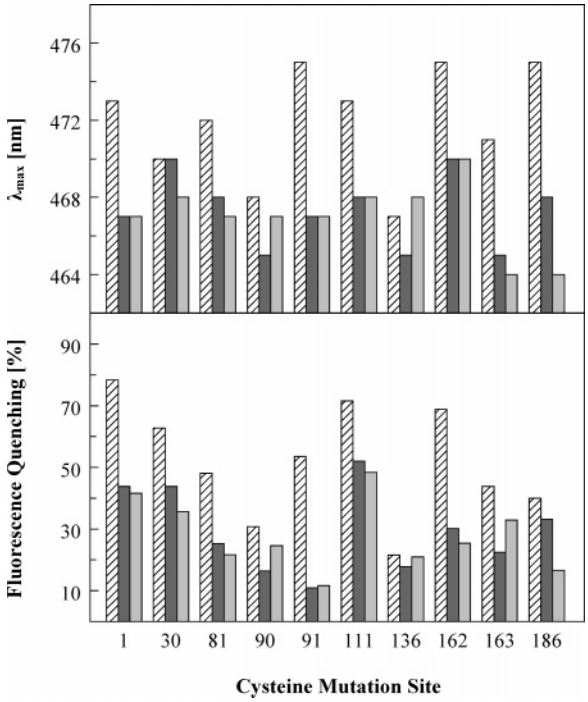

FIGURE 5: Bimane emission λ_{max} and BODIPY quenching of labeled A chain by anti-BODIPY antibody, with or without DMoPC/DOPG or DOPC/DOPG vesicles at pH 4.5. Top: emission λ_{max} of bimane fluorescence for 0.18 μM labeled A chain at pH 4.5 (striped bars) in solution or with SUVs composed of 400 μM (dark gray bars) 7:3 DMoPC/DOPG (mol/mol) or (light gray bars) 7:3 DOPC/DOPG (mol/mol). Bottom: anti-BODIPY antibody quenching of BODIPY fluorescence of 0.045 μM labeled A chain at pH 4.5 (striped bars) in solution or with SUVs composed of 100 μM 7:3 (dark gray bars) DMoPC/DOPG (mol/mol) or (light gray bars) 7:3 DOPC/DOPG (mol/mol). % quenching of fluorescence was calculated using the formula $(1 - F/F_0) \times 100\%$, where F is fluorescence after addition of anti-BODIPY antibody and F_0 is fluorescence in the absence of antibody.

reflect cases in which labeling decreases the stability of the folded state to a significant degree.

Bimane emission λ_{max} was also used to evaluate the location of different residues within the lipid bilayer. Several previous studies on T domain (*31*, *33*, *37*) have shown that the extent of the blue shift in bimane fluorescence λ_{max} will reflect the degree of burial of bimane residues within the hydrophobic core of a lipid bilayer. Figure 3B shows that the λ_{max} values at low pH in the presence of both DOPC/DOPG (light gray bars) and DMoPC/DOPG (dark gray bars) were significantly different from that in solution for all residues. In all cases, λ_{max} values were blue shifted relative to that in solution, indicating that the residues move into a more nonpolar location when the A chain is membrane-associated. This suggests that A chain residues all along the sequence interact with the lipid bilayer. Figure 5 (top) shows the absolute λ_{max} values for different bimane-labeled residues for samples prepared at pH 4.5 under the experimental conditions previously used to evaluate the topography of vesicle-inserted T domain (*24*, *31*, *33*). The λ_{max} values for bimane emission in DOPC/DOPG and DMoPC/DOPG vesicles (light and dark gray bars, respectively) were blue-shifted relative to those in solution (striped bars), in agreement with the pH titration data. Values in the presence of DOPC/DOPG and DMoPC/DOPG were similar, with the average bimane λ_{max} value in the presence of either lipid composition being about 467 nm. This value corresponds to relatively shallow insertion within the bilayer (*31*, *33*, *37*). Similar absolute values for the λ_{max} of bimane emission in these lipid mixtures at low pH were also obtained from the pH titration experiments (Figure 3, see caption).

A second method that we have used in a number of studies to evaluate the exposure of residues to solution is to measure the binding of externally added antibody to BODIPY-labeled Cys residues (*31*, *33*, *37*). Antibody can only bind to residues exposed to solution. The binding of anti-BODIPY antibodies to BODIPY-labeled residues can be detected by the quenching of BODIPY fluorescence. Previous studies using vesicle-inserted T domain have shown that the fluorescence of residues that are highly exposed to solution is generally quenched about 40−50% (*31*, *37*).

Strong quenching of BODIPY-labeled A chain residues by anti-BODIPY antibody confirms that most labeled-residues were highly exposed to solution in the absence of lipid (Figure 5 bottom, striped bars). In agreement with the bimane data, there was a decrease in exposure to solution in the presence of lipid vesicles and reactivity in the presence of DOPC-containing (light gray bars) and DMoPC-containing (dark gray bars) vesicles was similar.

The level of antibody binding to bilayer-bound A chain was very dependent upon the residue examined. Only three residues (1, 30, and 111) showed a high degree of antibody reactivity. The low level of reactivity was not due to insufficient antibody concentrations because control experiments on a number of samples showed that addition of excess antibody did not significantly increase quenching (data not shown). Weak quenching could mean that the other residues are inaccessible to antibody because they are somewhat deeply buried in the bilayer. On the other hand, these residues might be near the bilayer surface but located in a part of the protein that when lipid-bound has a local conformation that does not favor binding to antibody (*37*).

Measuring Depth of Penetration of Fluorescently-Labeled Residues by Fluorescence Quenching. Since the results of the antibody experiments were somewhat ambiguous, we decided to assay the depth of residue membrane penetration more directly. To do this, we developed a new fluorescence quenching assay. In previous studies, we used the parallax analysis fluorescence quenching approach to measure the depth of bimane-labeled residues within lipid bilayers (*31*). However, we found that the results were relatively variable. In a recent report, we demonstrated that the ratio of fluorescence quenching by the aqueous quencher acrylamide to that by 10-doxylnonadecane (10-DN), a membrane-embedded quencher, could be used to measure the depth of Trp residues within a bilayer (*26*). Because acrylamide cannot quench a wide variety of fluorescent groups, we modified this approach for use with bimane by choosing iodide as an aqueous quencher of fluorescence.

Quenchings of bimane-labeled T domain residues previously identified as inserting shallowly or deeply into lipid bilayers were used as standards to calibrate this method. Previous studies showed that T domain residues 322 and 378 insert shallowly in both DOPC/DOPG and DMoPC/DOPG SUVs, residue 361 inserts deeply in both types of SUVs, and residue 356 inserts shallowly in DOPC/DOPG SUVs but deeply in DMoPC/DOPG SUVs (*33*, *37*). As shown in Figure 6, quenching by iodide is strong for the appropriate

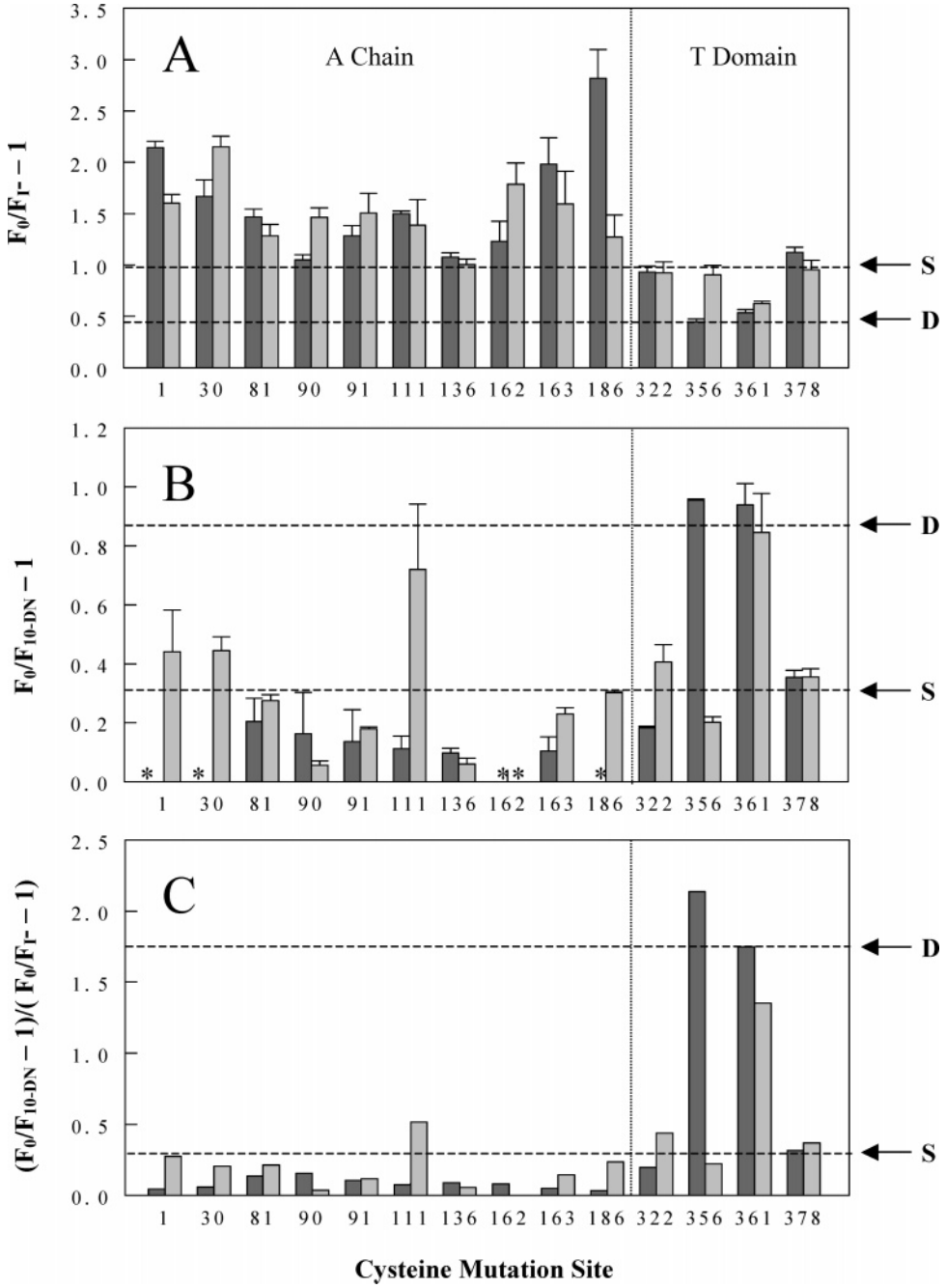

FIGURE 6: Iodide and 10-DN quenching of bimane fluorescence of labeled A chain and T domain in the presence of DMoPC/DOPG or DOPC/DOPG vesicles at pH 4.5. (A) iodide quenching of bimane fluorescence of vesicle-inserted labeled A chain or T domain. Samples contained 0.18 μM A chain or 0.20 μM T domain incorporated into SUVs composed of 400 μM (dark shaded bars) 7:3 DMoPC/DOPG (mol/mol) or (lightly shaded bars) 7:3 DOPC/DOPG at pH 4.5 with and without 100 mM KI. F_0/F_{I-} is the ratio of fluorescence in the absence of quencher (F_0) to that in the presence of quencher (F_{I-}) after correction for dilution with iodide. The average from two or three samples and standard deviations are shown. (B) 10-doxylnonadecane (10-DN) quenching of bimane fluorescence of vesicle-inserted labeled A chain or T domain. Samples contained 0.18 μM A chain or 0.20 μM T domain incorporated into SUVs composed of 400 μM (dark shaded bars) 7:3 DMoPC/DOPG (mol/mol) or (lightly shaded bars) 7:3 DOPC/DOPG with or without 7.2 mol % (for DMoPC/DOPG) or 9.1 mol % (for DOPC/DOPG) 10-DN at pH 4.5. F_0/F_{10-DN} is the ratio of fluorescence in the absence of quencher (F_0) to that in the presence of quencher (F_{10-DN}). Asterisk indicates samples in which quenching was not detected within experimental error. (C) ratio of quenching by 10-DN to that by iodide. An upper limit to the quenching ratio for residues in which 10-DN quenching was not significant (see B) was calculated assuming $F_0/F_{10-DN} - 1 = 0.1$. Dashed lines: calibration lines derived from the (approximate) averages of high and low quenching values (as indicated on right of figure) for residues previously shown to located deeply (D) and shallowly (S) in membrane-inserted T domain. Residues 322 and 378 are shallowly located in both DMoPC- and DOPC-containing vesicles. Residue 356 is shallowly located only in DOPC-containing vesicles (*33*, *37*).

T domain residues and conditions in which insertion is shallow (Figure 6A), whereas quenching by 10-DN shows the opposite pattern (Figure 6B). The ratio of 10-DN quenching to iodide quenching, which should give a more reliable assessment of membrane penetration depth than values from individual quenchers (*26*), also follows the expected pattern, i.e., a high ratio for deeply inserted residues and a low ratio for shallowly inserted ones (Figure 6C).

Comparison of quenching of bimane-labeled A chain to that of T domain residues clearly shows that in vesicle-

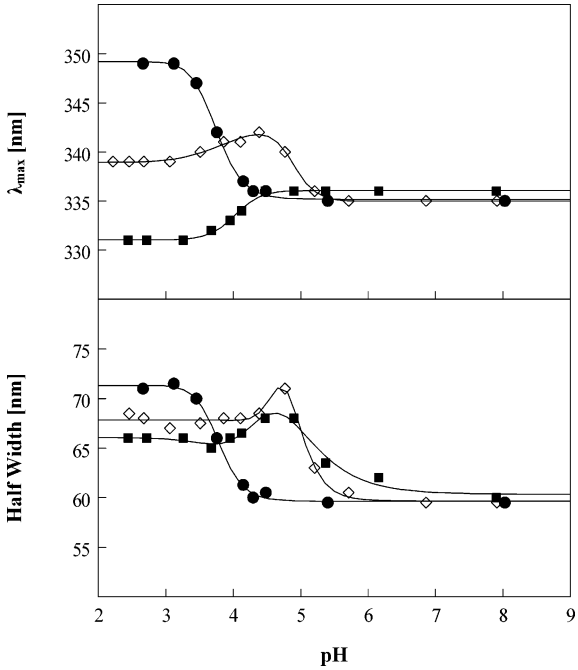

FIGURE 7: pH titration of native Trp fluorescence of Cys-less A chain with or without lipid vesicles. Top: pH dependence of λ_{max} of native Trp fluorescence. Bottom: pH dependence of native Trp fluorescence emission spectral peak width at half-maximal intensity. Samples contained 0.18 μM A chain (filled circles) in solution or in the presence of SUVs composed of 400 μM (open diamonds) 7:3 DMoPC/DOPG (mol/mol) or (filled squares) 7:3 DOPC/DOPG (mol/mol). Titration experiments performed as described in Figure 1. Several experiments using various unlabeled single Cys mutants exhibited λ_{max} titration curves in the presence of DOPC/DOPG and DMoPC/DOPG vesicles that were similar to that of the Cys-less protein (data not shown).

associated A chain, residues all along the A chain sequence are shallowly located within the lipid bilayer (Figures 6A and 6B). In general, this is true when iodide or 10-DN quenching is evaluated individually and when the 10-DN/iodide quenching ratio is examined (Figure 6C).

Differences Between A Chain Trp Fluorescence in DOPC/DOPG and DMoPC/DOPG Vesicles. We also monitored Trp fluorescence in order to see if the behavior of A chain inserted into DOPC/DOPG SUVs differed from that when inserted into DMoPC/DOPG SUVs. In view of the similarity of bimane fluorescence properties, it was surprising that this revealed drastic differences between Trp λ_{max} values for A chain inserted into these two types of lipid vesicles at low pH (Figure 7, top). At low pH in DOPC/DOPG vesicles (squares), there was a blue shift of Trp λ_{max} relative to that at neutral pH, consistent with movement of Trp into a more nonpolar environment, but in DMoPC/DOPG vesicles (diamonds), there was a red shift. Since the λ_{max} profiles with DMoPC/DOPG vesicles did not match those in the absence of lipid (Figure 7, top, circles), some factor other than a lack of association with lipid vesicles must have resulted in the red-shifted fluorescence observed in DMoPC/DOPG vesicles. A second unexpected result was that the apparent transition pH in DOPC/DOPG vesicles was significantly lower than that detected from bimane fluorescence and indeed lower than that detected in a previous study by quenching of Trp fluorescence (*11*). The transition seemed to occur at a pH similar to that for A chain in solution (Figure 7, top).

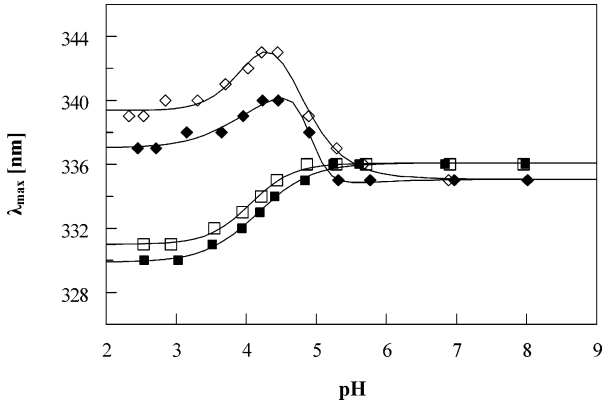

FIGURE 8: Effects of A chain concentration on pH titration profiles of native Trp fluorescence for Cys-less A chain in the presence of lipid vesicles. pH dependence of native Trp fluorescence of 0.09 μM (filled symbols) or 0.36 μM (open symbols) A chain in the presence of SUVs composed of 400 μM (diamonds) 7:3 DMoPC/DOPG (mol/mol) or (squares) 7:3 DOPC/DOPG (mol/mol). Titration experiments performed as described in Figure 1.

Previous studies have shown that oligomerization within lipid bilayers can strongly red-shift the fluorescence of Trp in membrane-inserted sequences (*41*, *42*). This could explain the behavior observed in the preceding experiments. If oligomerization was severe for A chain inserted into vesicles composed of DMoPC/DOPG, then a strong red shift might be expected. To try to see if oligomerization affects Trp λ_{max}, A chain concentration within the vesicles was increased. As seen in Figure 8, increasing A chain concentration increased the red shift in Trp fluorescence at low pH for A chain in DMoPC/DOPG vesicles (and to a small degree in DOPC/DOPG vesicles), consistent with an oligomerization-induced red shift.

The apparent shift in the transition pH in the DOPC/DOPG samples may also be an artifact of oligomerization. Measurement of emission peak half-widths, which increase when multiple species with different λ_{max} are present in a single sample (*26*, *43*), showed a maximum Trp peak width near pH 5 in the presence of both DOPC/DOPG and DMoPC/DOPG vesicles (Figure 7, bottom). This suggests that in both of these cases there was a conformational transition and lipid binding at pH 5, in agreement with bimane data and previous reports. We speculate that there is a greater degree of A chain oligomerization at pH 5 (presumably because the protein is close to its isoelectric point) relative to that at lower pH (where it should become progressively more cationic as pH is decreased). Near pH 5, the extent of A chain oligomerization (and the accompanying red shift) might be just enough in the DOPC/DOPG vesicles to cancel out the blue shift accompanying A chain insertion into the DOPC/DOPG vesicles. Extra strong oligomerization near pH 5 would also explain the observation that the red shift was strongest near pH 5 in samples containing DMoPC/DOPG vesicles (Figure 7, top). The red shift observed in DMoPC/DOPG vesicles at pH much lower than pH 5 may reflect an extent of oligomerization that is more than sufficient to obscure the blue shift that would be observed in the absence of oligomerization.

Chain-Induced Vesicle Fusion. Extensive A chain oligomerization within lipid vesicles was unexpected, as we used a protein/SUV ratio of between 2 and 4 protein molecules per SUV in most experiments (e.g., 1 protein:2300 lipid

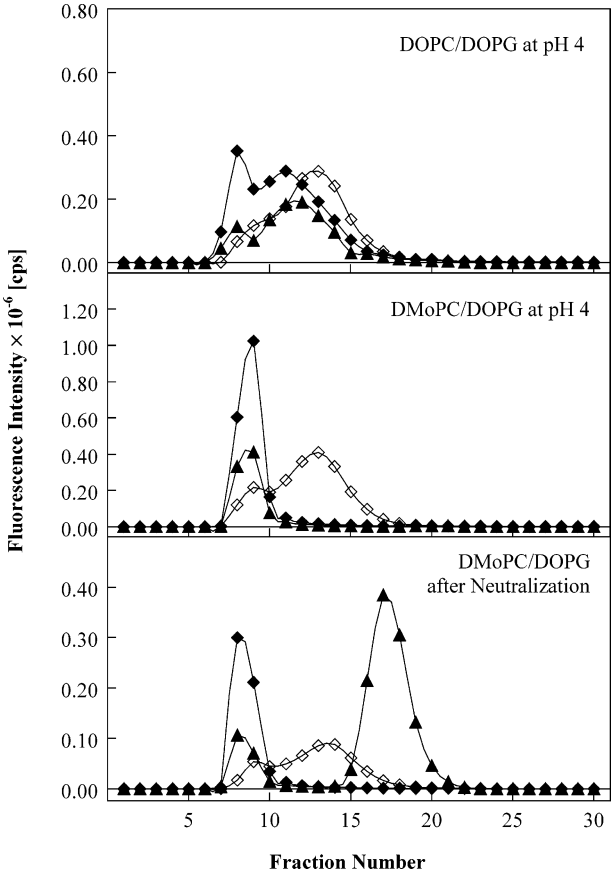

FIGURE 9: Gel filtration of Cys-less A chain mixed with vesicles at low pH and after neutralization of pH. Samples containing 0.5 mL of SUVs (9 mM lipid) with or without 20 μM Cys-less A chain were loaded onto a Sepharose 4B-CL column equilibrated at the sample pH. Filled diamonds: rhodamine-PE fluorescence in the presence A chain. Open diamonds: rhodamine-PE fluorescence in the absence of A chain. Filled triangles: Cys-less A chain Trp fluorescence. Top: gel-filtration profiles at pH 4 for trace rhodamine-PE-labeled 7:3 DOPC/DOPG (mol/mol) vesicles alone or mixed with Cys-less A chain. Middle: gel filtration profiles at pH 4 for rhodamine-PE labeled 7:3 DMoPC/DOPG (mol/mol) vesicles alone or mixed with Cys-less A chain. Bottom: gel-filtration profiles at pH 8 for samples prepared at pH 4 and then neutralized to pH 8 and containing rhodamine-PE labeled 7:3 DMoPC/DOPG (mol/mol) vesicles alone or mixed with A chain.

molecules in the topography experiments). However, a high degree of oligomerization would be possible if the A chain induced vesicle fusion, because fusion would increase the protein/vesicle ratio. To test this possibility, two techniques were used. The first was to examine apparent vesicle size by gel filtration. As seen in Figure 9(*middle* and *top*), at low pH, A chain fused or aggregated DMoPC/DOPG SUVs, whereas the size of DOPC/DOPG SUVs was little affected. Interestingly, as we previously demonstrated for DOPC-containing vesicles (*11*), neutralizing the pH induced dissociation of A chain from DMoPC-containing vesicles (about 86% dissociation as estimated from Trp fluorescence). However, the vesicles remained larger than their original size, which is more consistent with fusion than with vesicle aggregation arising from bound A chain.

Fluorescence energy transfer experiments using small amounts of donor (NBD-PE)- and acceptor (rhodamine-PE)-labeled vesicles tended to confirm vesicle fusion (*38*). In these experiments, a population of donor- and acceptor-labeled vesicles is mixed with a population of unlabeled vesicles. Fusion leads to a dilution of donor and acceptor and thus a loss in energy transfer. This assay gave results in agreement with the chromatography experiments. A chain at a protein-to-lipid mole ratio close to that used in the topography experiments (1:2300) induced dilution of labeled lipid in DMoPC-containing vesicles by 3.1-fold, whereas there was only a 1.5-fold dilution of labeled lipid in DOPC-containing vesicles (data not shown).

Table 1: Pore Formation Activity of Cys-less A Chain and T Domain at pH 4.5 Estimated from Leakage of Biocytin Entrapped in DMoPC/DOPG or DOPC/DOPG SUVs[a]

	$(F - F_0) \times 10^{-3}$ [cps][b]	
vesicles used	A chain	T domain
DMoPC/DOPG	57.2 ± 8.9	21.0 ± 1.3
DOPC/DOPG	5.2 ± 1.6	34.1 ± 4.6

[a] Samples contained SUVs composed of 200 μM 7:3 DMoPC/DOPG (mol/mol) or 7:3 DOPC/DOPG (mol/mol) with entrapped biocytin and were incubated with 0.09 μM A chain or 0.10 μM T domain in the presence of 0.05 μg/mL external BODIPY-labeled streptavidin at pH 4.5. [b] Difference between enhanced fluorescence of BODIPY-labeled streptavidin by biocytin in a sample containing protein (F) and fluorescence in a sample without protein (F_0) after 30 min of incubation. Values shown are the average and range for duplicate experiments. Average F_0 value and standard deviation for all samples was (65.5 ± 2.6) × 10^{-3} "relative counts per second" [cps]. After 90 min, there was a significant increase in fluorescence in the A chain samples in the presence of DMoPC/DOPG but not in the other samples. Addition of a second aliquot with twice the protein concentration as that in the first aliquot induced a further increase in fluorescence in all samples except those containing A chain in the presence of DOPC/DOPG vesicles. In the absence of protein, the leakiness of both DMoPC/DOPG and DOPC/DOPG vesicles to biocytin was very low, with an increase of BODIPY fluorescence in 90 min of less than 3.0 and 1.4%, respectively.

Pore Formation by Cys-less A Chain and T Domain at Low pH. Pore formation by the A chain was also examined. Since the A chain is hydrophilic, it might be predicted that deep A chain insertion would be associated with pore formation. To test for pore formation, we prepared SUVs in the presence of biocytin (biotinylated lysine), a small (M_r: 372.5) membrane-impermeable molecule (*44*), and detected biocytin leakage by an increase in BODIPY fluorescence induced by binding of biocytin to externally added BODIPY-streptavidin (*44*).

In these experiments, Cys-less A chain or T domain was externally added to SUVs containing entrapped biocytin at pH 4.5. As shown in Table 1, for DOPC/DOPG SUVs, A chain did not form a pore large enough to allow much leakage of entrapped biocytin. T domain, which is a pore-forming molecule (*45*), did induce extensive leakage of entrapped biocytin from DOPC/DOPG SUVs. In contrast, for DMoPC/DOPG vesicles both A chain and T domain induced continuous leakage of biocytin. It is noteworthy that A chain-induced biocytin leakage seems to accompany vesicle fusion, a process in which lipid bilayer integrity is transiently destabilized. This suggests that A chain-induced biocytin leakage in DMoPC-containing vesicles was due to vesicle fusion.

Permeability of Iodide Ion Through Lipid Bilayers Tested by NBD Fluorescence Quenching of Internally Labeled Vesicles. One important question about iodide is whether it only quenched bimane residues exposed to the external solution, or whether it might have also quenched bimane

residues exposed to the internal aqueous vesicle lumen. The observation that DMoPC-containing vesicles were leaky indicated that they would be permeable to iodide. To examine the permeability of iodide ions in the case of the DOPC-containing vesicles, we made NBD-PE-labeled 70% DOPC/30% DOPG SUVs and selectively destroyed the external NBD fluorescence with dithionite. This reagent converts the NBD nitro to an amine, creating the nonfluorescent ABD-PE (*40*). After the elimination of external NBD fluorescence (as expected for reduction of NBD in the external leaflet of SUVs, close to 2/3 of the fluorescence intensity was lost upon addition of dithionite (not shown)), we added iodide ion to quench NBD fluorescence (*46*). At pH 8, dithionite-treated SUVs, which are only internally NBD-labeled, showed 43% less iodide quenching of NBD compared with that of symmetrically NBD-labeled SUVs (i.e., prepared without dithionite treatment so that NBD groups are both in the inner and outer leaflets), indicating that iodide was not *fully* permeable at pH 8. However, at pH 4.5, the degree of quenching for the internally labeled SUVs was comparable with that of the symmetrically labeled SUVs (data not shown). This indicated that iodide ion could quench groups on both sides of DOPC-containing SUVs under the conditions used in the quenching experiments.

DISCUSSION

Topography of Vesicle-Inserted A Chain. Previous studies demonstrated that the isolated A chain (i.e., A chain in the absence of the remainder of diphtheria toxin) is able to interact with lipid vesicles via both electrostatic and hydrophobic interactions (*11*). We subsequently pointed out that there are β-strands in the A chain (CB4, CB5, CB6, and CB8) with a pattern similar to that found in transmembrane (TM) β-sheets, in which hydrophilic and hydrophobic residues are found in alternating positions (*23*). These observations, combined with the ability of the A chain to interact with micelles formed by a mild detergent (*11*), suggested the possibility that some part of isolated A chain inserted deeply into membranes, perhaps even forming TM β-strands under some conditions (*23*). The results in this study indicate that the isolated A chain does not insert very deeply into the bilayer. Shallow insertion was observed for residues within CB4 (residue 81), CB5 (residues 90, 91), CB6 (residue 136), and CB8 (residues 162, 163). In addition, residues close to the N- (residues 1, 30) and C-termini (residue 186) inserted shallowly. However, these results do not rule out the possibility that these sequences form a deeply inserted structure when associated with the remainder of DT.

The conclusions above assume that the secondary structure of the membrane-inserted A chain is similar to that of the A chain in solution. However, the secondary structure of A chain inserted into model membranes may be slightly different from that which it has in solution. By circular dichroism (CD), we found that the α-helix content increased from 9% in the native conformation to 23% in the presence of DOPC/DOPG vesicles at pH 4.5, while the content of the β-sheet decreased from about 36 to 27% (data not shown). In contrast, Wolff et al. (*47*) reported an increase in β-structure and none in α-helix upon A chain interaction with lipid vesicles at low pH using FTIR. It should be noted that the FTIR spectra at neutral pH seem to indicate secondary structure contents that are more similar to the crystal structure than those we obtained by CD (*2*, *48*). That might suggest that for the A chain, FTIR is more reliable than CD. On the other hand, the difference in lipid composition (DOPC/DOPG vs asolectin, a soy lipid mixture), vesicle type, A chain concentration, or buffer may be responsible for the differences between our results and those of Wolff et al. for membrane-associated A chain. For example, Wolff et al. used a higher A chain concentration in terms of protein/lipid ratio than that used in this study (1:8 vs 1:20 w/w) and used LUV. Combined, these factors would greatly increase the protein/vesicle ratio and might promote oligomerization, which could affect the secondary structure. In any case, the changes in secondary structure upon membrane insertion are not large.

Comparison of Fluorescence-Derived A Chain Topography to That Determined by Proteolysis and Photolabeling. In a very recent report, Wolff et al. carried out a proteolysis study of isolated A chain topography (*47*). In general terms, most of their proteolysis results are consistent with our study, as they concluded that most of the A chain was only inserted shallowly into lipid bilayers on the basis of the observation that many sites were exposed to protease added to the outside of the lipid bilayers. However, there are some important differences between their topographical model for the A chain and that in this report. First, Wolff et al. proposed that residues 134−151, which include much of CB6 and all of β-strand CB7, insert in the form of a TM β-sheet hairpin. We found that residue 136, which is in the center of a region of alternating hydrophobic and hydrophilic residues that overlaps β-strand CB6, locates shallowly in the bilayer, and this is not consistent with a TM hairpin. The idea that residues 134−151 form a TM hairpin also seems unlikely because CB7 differs from TM β-strands in known β-sheet membrane proteins by not having hydrophobic residues in alternating positions. If the sequence between 134 and 151 formed a TM β-hairpin, it would be very hydrophilic. Furthermore, known TM β-sheet proteins show that monomeric β-hairpins cannot form a stable TM β-barrel (*49*, *50*). TM β-barrel formation would require a significant degree of A chain oligomerization. A degree of oligomerization sufficient to form a β-barrel is not consistent with our data in DOPC-containing bilayers. In addition, TM β-barrels often form pores, and the inability of A chain to release biocytin in DOPC-containing vesicles is not consistent with pore formation.

A second difference is that our fluorescence studies suggest that residues 111, 162, 163, and 186 interact with lipid. Proteolysis data suggested that these residues were located in segments that are more exposed to solution than other A chain segments. Finally, on the basis of proteolysis, it was suggested that residues 77−100 equilibrate between a TM and surface topography. Our data on residues 90 and 91 indicate that insertion of this segment of the protein is as shallow as other parts of the A chain.

Some of the differences between the conclusions of Wolff et al. and those of this report may reflect ambiguities in interpretation of proteolysis studies. For example, when a protease cleaves at multiple sites in a single protein molecule, early cleavage events may perturb the protein conformation and thus alter the accessibility of sites to later proteolysis events. In fact, under conditions of limiting proteolysis, one may simply observe the membrane insertion propensities of

relatively short residual undigested polypeptides. It is also possible that the protease-resistant segments of the A chain are shallowly located but slightly more deeply inserted than other segments of the A chain, have a local conformation that is sufficient to confer protection from proteolysis, or are simply more tightly bound to vesicles than other segments of the A chain. The latter factor could explain the proteolysis pattern if proteolysis can only occur during transient periods in which individual A chain segments dissociate from the lipid bilayer while the remainder of the protein remains lipid-bound.

Of course, fluorescent probes may also be perturbing. However, previous studies have shown that the conclusions obtained with bimane-labeled toxin can be confirmed using other labeling groups, i.e., Trp residues introduced by mutagenesis, and by pore formation properties of unlabeled proteins (*34*, *51*). In addition, studies of bimane-labeled lysozyme have indicated that the bimane labels do not greatly perturb local protein conformation (*52*). In any case, most of our fluorescence data and the proteolysis data of Wolff et al. are consistent. Apparent differences may just reflect additional details derived from the present study.

Photolabeling studies of D'Silva and Lala have also investigated A chain topography (*53*). They reported that in whole DT, A chain residues 134−141 were labeled by hydrophobic photolabeling agents dissolved within the lipid bilayer. Unlike known TM β-strands, these residues did not seem to be exposed to an alternating hydrophobic/hydrophilic environment.

Although photolabeling experiments did not reveal the exact depth of these residues within the bilayer or unambiguously reveal their topography, they do suggest this labeled segment might insert more deeply than other segments of the A chain. This is not inconsistent with the conclusions from our data, especially because photolabeling studies were carried out on whole DT, and it is possible that the interaction of the A chain with the T domain of the toxin alters its topography and exposure to lipid. It remains possible that some β-strands do form TM structures at some point in the translocation process.

Comparison of A Chain Behavior in DMoPC-Containing Vesicles and DOPC-Containing Vesicles. It is also interesting that A chain topography was similar in DMoPC- and DOPC-containing vesicles, with shallow insertion observed in both types of vesicles. This is in contrast to the case of the T domain, in which bilayer width affects topography, such that T domain insertion is much deeper in SUVs containing DMoPC, a lipid with short 14-carbon acyl chains, than it is in SUVs containing DOPC, which has 18-carbon acyl chains (*33*). The difference between T domain and A chain behavior might reflect the A chain having a lesser ability to penetrate into the bilayer and form TM structures.

However, there were some differences between the behavior of the A chain in these two types of lipid mixtures. The A chain tended to induce fusion of DMoPC-containing SUVs but not DOPC-containing SUVs. Associated with this was a much greater tendency for the A chain to release trapped molecules from DMoPC vesicles. This difference might reflect a lesser stability of DMoPC-containing SUVs. Fusion may also help explain the apparent difference in A chain oligomerization in DMoPC-containing and DOPC-containing vesicles. Under the experimental conditions used, the concentration of A chains used was on the order 1 per 2000 lipids. This means there should be, on the average, 2−4 A chain molecules per SUV, which would preclude extensive oligomerization. However, upon fusion the A chain/vesicle ratio would increase, and this would make it possible for there to be a greater level of oligomerization. Thus, it is possible that the A chain has a significant tendency to oligomerize and could do so in DOPC-containing vesicles if there were a significant number of A chains per vesicle. In fact, in experiments in which pH titration was carried out at the same protein/lipid ratio in large unilamellar vesicles (LUVs) composed of DOPC/DOPG, A chain Trp fluorescence red-shifted at low pH in a manner similar to that observed when A chain was bound to DMoPC/DOPG SUVs (data not shown). This suggests that isolated A chain will oligomerize in bilayers at low pH when there are a sufficient number of protein molecules per vesicle. This is noteworthy because it may explain our previous observation that isolated A chain trapped within the lumen of PC/DOPG LUV was released at pH 4.3 (*7*). Those experiments used a high ratio of A chain molecules per vesicle, which may have induced fusion and a general leakiness of the lipid bilayer.

Advantages and Limitations of Use of 10-Doxylnonadecane/Iodide Quenching Ratio for Estimation of Fluorophore Depth. Fluorescence quenching was used to confirm the conclusions based on bimane λ_{max}. To do this, we modified a dual quencher method that we recently introduced for Trp residues (*26*), substituting iodide for acrylamide. In the dual quencher method, the depth of a fluorescent group within the lipid bilayer is estimated from the ratio of quenching by an aqueous quencher to that by one buried within the lipid bilayer. A quenching ratio is used to evaluate fluorophore depth rather than the quenching by a single quencher group because it helps cancel out factors that affect quenching other than depth. Such factors include the excited-state lifetime of the fluorescence group. A longer lifetime increases the sensitivity of a fluorophore to a quencher. Another such factor is the burial of a fluorescent group within a protein, which would tend to decrease sensitivity to quenching by an individual quencher (*54*).

The limitations of quenching experiments should also be mentioned. The fact that iodide is anionic means that electrostatic interactions could also affect the level of iodide quenching. This should be kept in mind, especially when comparing results in lipid bilayers with different electric charge, but could also be a factor when a fluorescent group is located near a highly charged section of a protein. The observation that the individual quenching values observed for 10-DN (which is uncharged) and iodide were generally consistent with each other, and with the λ_{max} values, suggests that electrostatic effects were not a problem in the present study. In addition, the reliability of the quenching data is supported by the observation that the quenching values obtained for T domain residues were consistent with the depths previously estimated by other methods (*33*, *37*). Nevertheless, identification of an uncharged aqueous quencher that could be used with a wide variety of fluorophores would be highly desirable. Interpretation of quenching was also limited by the lack of a precise calibration of the quenching ratio based on bimane-labeled residues of exactly known depth. This was not critical for the present study,

but a more exact calibration is necessary to obtain more exact estimates of bimane depth.

CONCLUSION

Implications for A Chain Translocation. Combining the results of this study with those obtained by proteolysis indicates that most of the A chain inserts so that it is associated with the surface of the bilayer at low pH. Thus, the interaction of the A chain with the T domain of the toxin is likely to be necessary for A chain translocation in vivo. We cannot be certain if or when during the translocation process the A chain is partly or fully exposed to lipid. For example, the hydrophobic behavior of the unfolded A chain may be important because the T domain acts as a chaperone (*12*), not because it imparts the ability to bind lipid, and the A chain might not be exposed to lipid during translocation. On the other hand, even if the T domain acts as a chaperone, it is possible that the A chain is somewhat exposed to lipid prior to interaction with the T domain or during the translocation step. This would explain the accessibility of the A chain to hydrophobic photolabeling agents in whole DT. Future studies of the topography of the A chain during the translocation process should reveal which (if any) of these models is correct.

REFERENCES

1. Choe, S., Bennett, M. J., Fujii, G., Curmi, P. M., Kantardjieff, K. A., Collier, R. J., and Eisenberg, D. (1992) The crystal structure of diphtheria toxin *Nature 357*, 216−222.
2. Bennett, M. J., and Eisenberg, D. (1994) Refined structure of monomeric diphtheria toxin at 2.3 Å resolution *Protein Sci. 3*, 1464−1475.
3. Ratts, R., Zeng, H., Berg, E. A., Blue, C., McComb, M. E., Costello, C. E., vanderSpek, J. C., and Murphy, J. R. (2003) The cytosolic entry of diphtheria toxin catalytic domain requires a host cell cytosolic translocation factor complex *J. Cell Biol. 160*, 1139−1150.
4. Pappenheimer, A. M., Jr. (1977) Diphtheria toxin *Annu. Rev. Biochem. 46*, 69−94.
5. Umata, T., and Mekada, E. (1998) Diphtheria toxin translocation across endosome membranes. A novel cell permeabilization assay reveals new diphtheria toxin fragments in endocytic vesicles *J. Biol. Chem. 273*, 8351−8359.
6. Oh, K. J., Senzel, L., Collier, R. J., and Finkelstein, A. (1999) Translocation of the catalytic domain of diphtheria toxin across planar phospholipid bilayers by its own T domain *Proc. Natl. Acad. Sci. U.S.A. 96*, 8467−8470.
7. Jiang, J. X., Chung, L. A., and London, E. (1991) Self-translocation of diphtheria toxin across model membranes *J. Biol. Chem. 266*, 24003−24010.
8. Beaumelle, B., Bensammar, L., and Bienvenue, A. (1992) Selective translocation of the A chain of diphtheria toxin across the membrane of purified endosomes *J. Biol. Chem. 267*, 11525−11531.
9. Papini, E., Schiavo, G., Tomasi, M., Colombatti, M., Rappuoli, R., and Montecucco, C. (1987) Lipid interaction of diphtheria toxin and mutants with altered fragment B. 2. Hydrophobic photolabelling and cell intoxication *Eur. J. Biochem. 169*, 637−644.
10. London, E. (1992) Diphtheria toxin: membrane interaction and membrane translocation *Biochim. Biophys. Acta 1113*, 25−51.
11. Zhao, J. M., and London, E. (1988) Conformation and model membrane interactions of diphtheria toxin fragment A *J. Biol. Chem. 263*, 15369−15377.
12. Ren, J., Kachel, K., Kim, H., Malenbaum, S. E., Collier, R. J., and London, E. (1999) Interaction of diphtheria toxin T domain with molten globule-like proteins and its implications for translocation *Science 284*, 955−957.
13. Hammond, K., Caputo, G. A., and London, E. (2002) Interaction of the membrane-inserted diphtheria toxin T domain with peptides and its possible implications for chaperone-like T domain behavior *Biochemistry 41*, 3243−3253.
14. Boquet, P., Silverman, M. S., Pappenheimer, A. M., Jr., and Vernon, W. B. (1976) Binding of Triton X-100 to diphtheria toxin, crossreacting material 45, and their fragments *Proc. Natl. Acad. Sci. U.S.A. 73*, 4449−4453.
15. Drazin, R., Kandel, J., and Collier, R. J. (1971) Structure and activity of diphtheria toxin. II. Attack by trypsin at a specific site within the intact toxin molecule *J. Biol. Chem. 246*, 1504−1510.
16. Hu, V. W., and Holmes, R. K. (1984) Evidence for direct insertion of fragments A and B of diphtheria toxin into model membranes *J. Biol. Chem. 259*, 12226−12233.
17. Montecucco, C., Schiavo, G., and Tomasi, M. (1985) pH-dependence of the phospholipid interaction of diphtheria-toxin fragments *Biochem. J. 231*, 123−128.
18. Zalman, L. S., and Wisnieski, B. J. (1984) Mechanism of insertion of diphtheria toxin: peptide entry and pore size determinations *Proc. Natl. Acad. Sci. U.S.A. 81*, 3341−3345.
19. Cabiaux, V., Brasseur, R., Wattiez, R., Falmagne, P., Ruysschaert, J. M., and Goormaghtigh, E. (1989) Secondary structure of diphtheria toxin and its fragments interacting with acidic liposomes studied by polarized infrared spectroscopy *J. Biol. Chem. 264*, 4928−4938.
20. Jiang, J. X., Abrams, F. S., and London, E. (1991) Folding changes in membrane-inserted diphtheria toxin that may play important roles in its translocation *Biochemistry 30*, 3857−3864.
21. Falnes, P. O., Choe, S., Madshus, I. H., Wilson, B. A., and Olsnes, S. (1994) Inhibition of membrane translocation of diphtheria toxin A-fragment by internal disulfide bridges *J. Biol. Chem. 269*, 8402−8407.
22. Falnes, P. O., and Olsnes, S. (1995) Cell-mediated reduction and incomplete membrane translocation of diphtheria toxin mutants with internal disulfides in the A fragment *J. Biol. Chem. 270*, 20787−20793.
23. Tortorella, D., Sesardic, D., Dawes, C. S., and London, E. (1995) Immunochemical analysis shows all three domains of diphtheria toxin penetrate across model membranes *J. Biol. Chem. 270*, 27446−27452.
24. Kachel, K., Asuncion-Punzalan, E., and London, E. (1998) The location of fluorescence probes with charged groups in model membranes *Biochim. Biophys. Acta 1374*, 63−76.
25. Haugland, R. P. (2002) *Handbook of Fluorescent Probes and Research Chemicals*, 9th ed., Molecular Probes, Eugene, OR.
26. Caputo, G. A., and London, E. (2003) Using a novel dual fluorescence quenching assay for measurement of tryptophan depth within lipid bilayers to determine hydrophobic α-helix locations within membranes *Biochemistry 42*, 3265−3274.
27. Caputo, G. A., and London, E. (2004) Position and ionization state of Asp in the core of membrane-inserted α helices control both the equilibrium between transmembrane and nontransmembrane helix topography and transmembrane helix positioning *Biochemistry 43*, 8794−8806.
28. Barbieri, J. T., and Collier, R. J. (1987) Expression of a mutant, full-length form of diphtheria toxin in *Escherichia coli Infect. Immun. 55*, 1647−1651.
29. Greenfield, L., Bjorn, M. J., Horn, G., Fong, D., Buck, G. A., Collier, R. J., and Kaplan, D. A. (1983) Nucleotide sequence of the structural gene for diphtheria toxin carried by corynebacteriophage *β Proc. Natl. Acad. Sci. U.S.A. 80*, 6853−6857.
30. Ren, J., Sharpe, J. C., Collier, R. J., and London, E. (1999) Membrane translocation of charged residues at the tips of hydrophobic helices in the T domain of diphtheria toxin *Biochemistry 38*, 976−984.
31. Rosconi, M. P., and London, E. (2002) Topography of helices 5−7 in membrane-inserted diphtheria toxin T domain: identification and insertion boundaries of two hydrophobic sequences that do not form a stable transmembrane hairpin *J. Biol. Chem. 277*, 16517−16527.
32. Sambrook, J., Fritsch, E. I., Maniatis, T. (1989) *Molecular Cloning*, 2nd ed., Cold Spring Harbor Press, Plainview, NY.
33. Wang, Y., Malenbaum, S. E., Kachel, K., Zhan, H., Collier, R. J., and London, E. (1997) Identification of shallow and deep membrane-penetrating forms of diphtheria toxin T domain that are regulated by protein concentration and bilayer width *J. Biol. Chem. 272*, 25091−25098.
34. Malenbaum, S. E., Collier, R. J., and London, E. (1998) Membrane topography of the T domain of diphtheria toxin probed with single tryptophan mutants *Biochemistry 37*, 17915−17922.
35. Bradford, M. M. (1976) A rapid and sensitive method for the quantitation of microgram quantities of protein utilizing the principle of protein−dye binding *Anal. Biochem. 72*, 248−254.

36. Pace, C. N., Vajdos, F., Fee, L., Grimsley, G., and Gray, T. (1995) How to measure and predict the molar absorption coefficient of a protein *Protein Sci. 4*, 2411−2423.
37. Kachel, K., Ren, J., Collier, R. J., and London, E. (1998) Identifying transmembrane states and defining the membrane insertion boundaries of hydrophobic helices in membrane-inserted diphtheria toxin T domain *J. Biol. Chem. 273*, 22950−22956.
38. Tortorella, D., Ulbrandt, N. D., and London, E. (1993) Simple centrifugation method for efficient pelleting of both small and large unilamellar vesicles that allows convenient measurement of protein binding *Biochemistry 32*, 9181−9188.
39. Cabrita, L. D., Whisstock, J. C., and Bottomley, S. P. (2002) Probing the role of the F-helix in serpin stability through a single tryptophan substitution *Biochemistry 41*, 4575−4581.
40. McIntyre, J. C., and Sleight, R. G. (1991) Fluorescence assay for phospholipid membrane asymmetry *Biochemistry 30*, 11819−11827.
41. Ren, J., Lew, S., Wang, J., and London, E. (1999) Control of the transmembrane orientation and interhelical interactions within membranes by hydrophobic helix length *Biochemistry 38*, 5905−5912.
42. Lew, S., Caputo, G. A., and London, E. (2003) The effect of interactions involving ionizable residues flanking membrane-inserted hydrophobic helices upon helix−helix interaction *Biochemistry 42*, 10833−10842.
43. Ren, J., Lew, S., Wang, Z., and London, E. (1997) Transmembrane orientation of hydrophobic α-helices is regulated both by the relationship of helix length to bilayer thickness and by the cholesterol concentration *Biochemistry 36*, 10213−10220.
44. Rosconi, M. P., Zhao, G., and London, E. (2004) Analyzing topography of membrane-inserted diphtheria toxin T domain using BODIPY-streptavidin: At low pH, helices 8 and 9 form a transmembrane hairpin but helices 5−7 form stable nonclassical inserted segments on the cis side of the bilayer *Biochemistry 43*, 9127−9139.
45. Zhan, H., Oh, K. J., Shin, Y. K., Hubbell, W. L., and Collier, R. J. (1995) Interaction of the isolated transmembrane domain of diphtheria toxin with membranes *Biochemistry 34*, 4856−4863.
46. Li, Q. T., and Kam, W. K. (1997) Steady-state fluorescence quenching for detecting acyl chain interdigitation in phosphatidylcholine vesicles *J. Biochem. Biophys. Methods 35*, 11−22.
47. Wolff, C., Wattiez, R., Ruysschaert, J. M., and Cabiaux, V. (2004) Characterization of diphtheria toxin's catalytic domain interaction with lipid membranes *Biochim. Biophys. Acta 1661*, 166−177.
48. Bennett, M. J., Choe, S., and Eisenberg, D. (1994) Refined structure of dimeric diphtheria toxin at 2.0 Å resolution *Protein Sci. 3*, 1444−1463.
49. Shatursky, O., Heuck, A. P., Shepard, L. A., Rossjohn, J., Parker, M. W., Johnson, A. E., and Tweten, R. K. (1999) The mechanism of membrane insertion for a cholesterol-dependent cytolysin: a novel paradigm for pore-forming toxins *Cell 99*, 293−299.
50. Hotze, E. M., Heuck, A. P., Czajkowsky, D. M., Shao, Z., Johnson, A. E., and Tweten, R. K. (2002) Monomer−monomer interactions drive the prepore to pore conversion of a β-barrel-forming cholesterol-dependent cytolysin *J. Biol. Chem. 277*, 11597−11605.
51. Zhan, H., Elliott, J. L., Shen, W. H., Huynh, P. D., Finkelstein, A., and Collier, R. J. (1999) Effects of mutations in proline 345 on insertion of diphtheria toxin into model membranes *J. Membr. Biol. 167*, 173−181.
52. Mansoor, S. E., McHaourab, H. S., and Farrens, D. L. (1999) Determination of protein secondary structure and solvent accessibility using site-directed fluorescence labeling. Studies of T4 lysozyme using the fluorescent probe monobromobimane *Biochemistry 38*, 16383−16393.
53. D'Silva, P. R., and Lala, A. K. (2000) Organization of diphtheria toxin in membranes. A hydrophobic photolabeling study *J. Biol. Chem. 275*, 11771−11777.
54. Ladokhin, A. S. (1999) Evaluation of lipid exposure of tryptophan residues in membrane peptides and proteins *Anal. Biochem 276*, 65−71.

BI0482093